Send Orders for Reprints to reprints@benthamscience.net

Current Medicinal Chemistry, **2014**, *21*, 113-123

In Vivo Imaging of the Metabotropic Glutamate Receptor 1 (mGluR1) with Positron Emission Tomography: Recent Advance and Perspective

Songye Li and Yiyun Huang*

PET Center, Department of Diagnostic Radiology, Yale University School of Medicine, New Haven, CT, USA

Abstract: The metabotropic glutamate 1 receptors (mGluR1) have been shown to play a role in neuropathic pain and neurological and psychiatric disorders such as ischemia, epilepsy, anxiety, as well as schizophrenia and other cognition-related disorders. As a result, mGluR1 has been an important target for drug development. As a radiotracer-based *in vivo* imaging technique Positron Emission Tomography (PET) is an important tool in the investigation of receptor function in the living brain under normal conditions and its dysfunction in diseases, as well as in the study of receptor occupancy by experimental therapeutic agents. In this report we review the development and evaluation of PET radiotracers for mGluR1 and provide an assessment of the tracers that are likely to succeed in the imaging and quantification of mGluR1 in humans.

Keywords: Metabotropic glutamate receptor, mGlu1, radioligand, positron emission tomography, synthesis, evaluation.

INTRODUCTION

The Glutamate Receptors

The endogenous ligand *L*-glutamate is a major excitatory neurotransmitter in the central nervous system (CNS) [1, 2]. Over the past three decades, glutamate receptors have been the focus of investigation on the pathophysiology of neurological and psychiatric disorders [3]. Two major types of receptors regulate glutamatergic neurotransmission in the brain, as defined by their mechanisms of activation and effect on postsynaptic current: ionotropic glutamate (iGlu) receptors, which form the ion channel pore that activates when glutamate binds to the receptor; and metabotropic glutamate (mGlu) receptors, which are coupled with heterotrimeric G-protein [4]. The mGlu receptors (mGluR) are composed of a family of eight receptor subtypes classified into three groups: group I (mGluR1 and 5), group II (mGluR2 and 3) and group III (mGluR4, 6, 7 and 8) [5]. This classification is based on the differences in receptor sequence homology, pharmacology, and signal transduction mechanism [6].

Distribution of mGluR1 in the Brain and Involvement in CNS Disorders

Group I mGlu receptors (mGluR1 and 5) are mainly postsynaptic receptors that are activated by 3,5-dihydroxyphenylglycine (3,5-DHPG). Although mGluR1 was the first to be cloned among the mGluR family [7, 8], investigation of its distribution in the brain was limited for a long time to in-situ hybridization or immunohistochemistry studies due to the lack of selective mGluR1 radioligands. Only in 2003, Lavreysen *et al.* reported the characterization of [^{3}H]R214127 as a selective antagonist radioligand for mGluR1, which allowed the detailed mapping of the mGluR1 in the rat brain by quantitative autoradiography and radioligand binding assays in brain tissues [9, 10]. The mGlu1 receptors are widely distributed in the brain, with high concentrations in the cerebellum, midbrain, thalamus and hypothalamus, intermediate levels in the striatum, hippocampus and cortex, and negligible levels in the medulla. The mGluR1 has been shown to play a role in neuropathic pain and neurological and psychiatric disorders such as ischemia, epilepsy, anxiety, as well as schizophrenia and other cognition-related disorders [11-14]. As a result, mGluR1 has been an important target for drug development [14, 15].

In Vivo Imaging of mGluR1

As a sensitive, non-invasive molecular imaging technique, Positron Emission Tomography (PET) enables the study of biochemical interaction in the living brain and, in particular, specific proteins involved in pathophysiology. In addition to its applications in the investigation of a receptor's density distribution and changes under neurological and psychiatric conditions, PET can also be used to assess novel therapeutic agents for target engagement and correlation of target occupancy and therapeutic effects [16-19]. Since mGluR1 has been implicated in a number of CNS disorders and targeted for drug development, there have been extensive search for effective PET imaging agents to investigate this receptor subtype *in vivo*.

In this review, we will survey the literature and describe the structure, synthesis, and characterization of PET imaging radioligands for mGluR1. Wherever available, *in vivo* imaging data will be compiled and appraised to gauge the potential of the radioligands for successful translation from preclinical to clinical applications.

*Address correspondence to this author at PET Center, Department of Diagnostic Radiology, Yale University School of Medicine, 801 Howard Avenue, PO Box 208048, New Haven, CT 06520-8048, USA;
Tel: (203)785-3193; Fax: (203)785-2994; E-mail: henry.huang@yale.edu

1875-533X/14 $58.00+.00

REQUIREMENTS FOR A PET RADIOTRACER

PET imaging relies on the availability of specific radioligands or tracers that bind selectively to a target receptor *in vivo*. In order to be an effective PET tracer for imaging a CNS receptor, a radioligand has to meet a demanding set of requirements. These requirements have been recognized by seasoned practitioners in the tracer development field and widely discussed in the literature [20-22]. They include: 1) radiochemistry feasibility, i.e., the possibility of using a limited steps of chemical transformations to incorporate into the biologically active molecule a short-lived positron emitting radioisotope, most commonly carbon-11 (radioactive decay half-life ($t_{1/2}$) of 20.4 min) and fluorine-18 ($t_{1/2}$ = 110 min) for CNS applications; 2) ability to cross the blood-brain barrier (BBB), i.e., appropriate lipophilicity for facile brain entry and low propensity for efflux by membrane transporters on the BBB; 3) adequate binding affinity and selectivity for the target receptor; 4) reasonable metabolic profiles *in vivo* without production of radioactive metabolites able to enter the brain and complicate the interpretation of imaging data; 5) appropriate *in vivo* pharmacology, i.e., displaying specific and saturable tissue binding; 6) appropriate pharmacokinetic profile in the brain with reversible binding characteristics observed within the usable time window of the radioisotope; 7) acceptable toxicology profile with no toxicity associated with the administration of the tracer; and 8) adequate specific binding signals *in vivo*. Obviously, the ultimate goal of PET imaging tracer development is to meet the last requirement of providing adequate specific binding signals *in vivo* to allow the effective visualization and reliable quantification of the target. All the other requisite properties are there to ensure the realization of this goal.

Based on *in vitro* measurements of a receptor's density, B_{max}, and a ligand's binding affinity to the target receptor, $1/K_D$, a numerical *in vitro* binding potential (*BP*), defined as $BP = B_{max}/K_D$, with a value of >10, has been advocated as the first order selection criterion to determine whether a ligand is able to provide measurable specific binding signal, and thus warranted to advance to *in vivo* evaluation [23, 24]. On the other hand, as illustrated by Eckelman *et al.* [25, 26], *in vitro* guidelines as such are helpful in eliminating, in the early stage of tracer development, ligands that are likely to fail *in vivo*. However, they are not sufficient to predict the likelihood that a tracer will provide adequate specific binding signals *in vivo*, because experiments *in vitro* are conducted in an idealized (*i.e.* free of interfering factors) and well-controlled environment, whereas in the *in vivo* environment, a tracer's systemic pharmacokinetic and pharmacodynamic parameters, such as delivery, distribution, metabolism, clearance, and binding to plasma proteins all come into play to impact upon the ability of a tracer to exhibit a reliably measurable signal [25, 26]. Thus in the *in vivo* situation, a tracer's specific binding signal is best defined by the term BP_{ND}, the specific to non-specific binding ratio at equilibrium, as in the equation below

$$BP_{ND} = f_{ND} * B_{avail} / K_D = f_p * B_{avail} / V_{ND} * K_D \quad (1)$$

Where f_{ND} is the fraction of free ligand in the non-displaceable tissue compartment, B_{avail} is the concentration of a receptor available for binding to the tracer, K_D is the tracer's equilibrium dissociation constant (inverse of binding affinity), f_p is the tracer's free fraction in the plasma, and V_{ND} is the distribution volume in the non-displaceable tissue compartment, as defined by Innis, *et al.* [27].

As illustrated by Equation 1, BP_{ND}, or the *in vivo* specific binding signal provided by a tracer, is determined by many factors. The concentration of the target protein in the region of interest, a tracer's binding affinity to the target, its free fraction in the plasma or brain tissue, and its binding to non-targets (non-specific binding, or non-displaceable binding) are all contributing factors. In summary, the density (B_{max}) of the target receptor in the brain determines the requisite affinity ($1/K_D$) of a ligand needed to visualize the targeted neuroreceptor, and the term "B_{max}/K_D" provides an initial roadmap for the selection of candidate ligands for PET imaging tracer development. More importantly, the term "f_p/V_{ND}", which can be broadly referred to as non-specific, or off-target binding, may be the deciding factor in the success or failure of a radioligand for *in vivo* imaging applications.

Laveraysen *et al.* have used the selective radioligand [^{3}H]R214127 to determine the densities of mGluR1 in selected brain regions in rat, while Hostetler *et al.* used the radioligand [^{18}F]MK-1312 to measure mGluR1 concentrations in the cerebellum and cortex of monkey and human [10, 28]. These regional B_{max} values are listed in Table **1**. Using these B_{max} values and a minimum B_{max}/K_D value of 10 for ligand selection, a K_D value of < 5 nM is required for labeling mGluR1 in the cerebellum in all species, and a minimum K_D of 2.6 nM is required for human cortex.

PET RADIOLIGANDS FOR THE mGlu1 RECEPTOR

In 2005, we reported the first PET radioligand for imaging mGluR1 in rats: [^{11}C]JNJ-16567083 (**1**) (Fig. **1**) [29]. It was derived from a large series of selective mGluR1 antagonists with a substituted quinoline skeleton and structurally related to the radioligand [^{3}H]R214127 [9, 30]. The radiolabeling precursor was prepared through a 3-step procedure

Table 1. Concentrations (B_{max}) of mGluR1 in Regions of Rat, Monkey and Human Brain

Species	Regional B_{max} (nM)			
	Cortex	Hippocampus	Striatum	Cerebellum
Rat	47.1 ± 6.8	68.8 ± 12.5	74.1 ± 4.8	430.2 ± 204.2
Rhesus monkey	10 ± 1.9	-	-	53 ± 12
Human	26 ± 15	-	-	82 ± 33

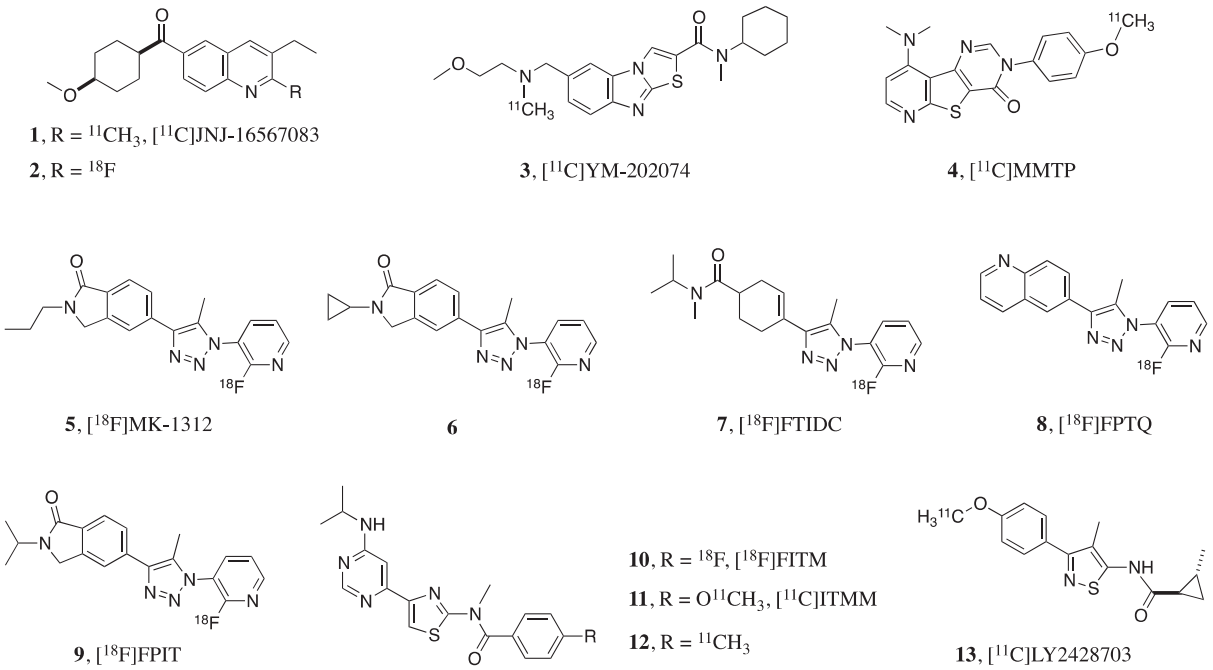

Fig. (1). PET radioligands for mGluR1.

starting from *N*-(4-bromophenyl)butanamide. Radioligand **1** was synthesized by Pd (0)-catalyzed Stille coupling of the aryltrimethyltin precursor with [^{11}C]methyl iodide (Fig. **2**). Decay-corrected radiochemical yield was 47% at the end of synthesis (EOS, based on [^{11}C]MeI). Radioligand **1** was shown to possess high affinity towards the rat mGluR1 (K_i = 0.87 nM), and about 3,000-fold selectivity over mGluR5. *Ex vivo* study showed high uptake in the cerebellum, striatum, hippocampus and frontal cortex. Binding of **1** in the cerebellum was reduced by 81% when the animals were pretreated with selective mGluR1 antagonists and remained unchanged during pretreatment with selective mGluR2 (LY341495) or mGluR5 (MPEP) antagonist, which clearly demonstrated the binding specificity and selectivity of this radioligand for mGluR1. *In vivo* micro-PET imaging experiments confirmed the specific binding in a living rat, and radioactivity entered the brain rapidly and localized to mGluR1-rich regions with peak uptake time of ~10 min.

We have also evaluated the F-18 labeled antagonist **2**, a close structural analog of **1**. Radioligand **2** was synthesized in 27% radiochemical yield (EOS, decay-corrected) through [^{18}F]fluorination of the 2-chloroquinoline precursor (Fig. **2**). In initial binding assays **2** displayed high affinities for the cloned rat mGlu1a (one of the five variants of mGluR1, which differ in the length of C-terminal tail) receptor and rat cerebellum membrane homogenates (K_i of 0.87 and 1.07 nM, respectively) [31]. *Ex vivo* biodistribution study in rats indicated the binding specificity and selectivity of **2** to mGluR1, despite the fact that its specific binding was lower than that of **1**. However, when evaluated in non-human primates later, both **1** and **2** were found to display little specific binding in the brain. In order to understand the discrepancy in specific binding signals between rodents and non-human primates, further binding assays were carried out using cloned human mGluR1 with incubation at body temperature (37 °C). As it turned out, the binding affinities of these two ligands were much lower for human mGluR1, and further reduced when assayed at body temperature vs. at 4 °C (Table **2**). Due to this affinity differences between species and temperatures, we concluded that radioligands **1** and **2** were not suitable for *in vivo* imaging of mGluR1 in primates.

A few years of inactivity ensued after the disclosure of the first attempt at developing a selective mGluR1 PET radioligand, then in 2010 Yanamoto *et al.* reported the synthesis and evaluation of [^{11}C]YM-202074 (**3**), in a structural skeleton completely different from that of **1** and **2**, with a benzoimidazoline ring fused with thiazoline (Fig. **1**) [32]. Radiosynthesis of [^{11}C]YM-202074 was accomplished in 7.4% radiochemical yield (based on [^{11}C]CO_2 at end of bombardment) by reaction of the secondary amine precursor with [^{11}C]MeI (Fig. **3**). This ligand possessed nanomolar binding affinity (K_i = 4.8 nM) and good selectivity, as well as suitable lipophilicity (log *D* of 2.7) (Table **2**). Autoradiography studies *in vitro* and *ex vivo* indicated that it bound to mGluR1. However, in PET imaging experiments in rats it displayed low brain uptake, low specific binding and a distribution pattern inconsistent with the regional densities of mGluR1. Apparently it cannot serve as a useful tracer. Given the high binding affinity and optimal lipophilicity of this radiotracer, these *in vivo* results were somewhat unexpected and might be attributed to the rapid metabolism of the ligand and entry of radioactive metabolites into the brain. Indeed, in metabolism studies in mice only ~5% of the parent tracer remained in the plasma at 30 min post-injection. Further, at the same time point the parent tracer accounted for only ~50% of the radioactivity in the cerebellum, and ~10% in the rest of the brain.

Another PET radioligand for mGluR1, [^{11}C]MMTP (**4**) (Fig. **1**), was reported in 2010 by Prabhakaran *et al.* [33]. This ligand also had nanomolar affinity (K_i = 7.9 nM) and selectivity of >1,000 times for mGluR1 over mGluR5

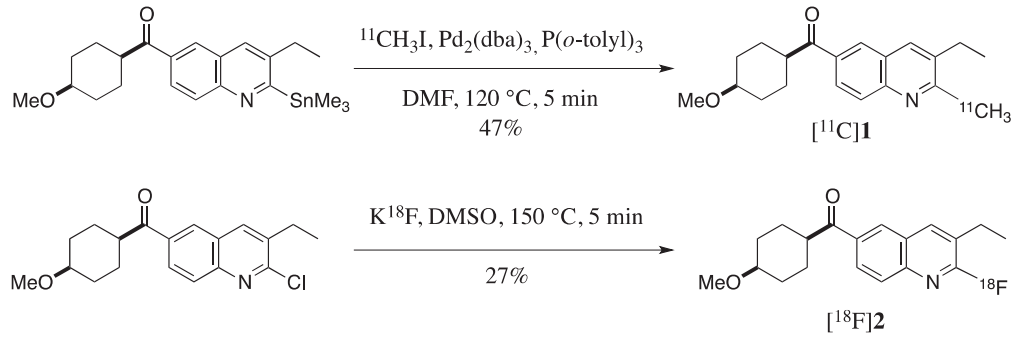

Fig. (2). Radiosynthesis of [^{11}C]**1** and [^{18}F]**2**.

Table 2. Affinity and Lipophilicity of PET Radioligands for mGlu1 Receptors

Radioligand	Binding affinity (nM)		Membrane	Assay Temperature	Measured log *P* (log *D*)	PET Species
	K_i	IC_{50}				
1 [^{11}C]JNJ-16567083	0.87 ± 0.43 [a]	-	Cloned rat mGluR1	4 °C	3.38 [31]	Rat & Baboon
	0.57 ± 0.41 [a]	-	Rat cerebellum homogenate			
	4.75 ± 0.70 [a]	-	Cloned human mGluR1			
	3.49 ± 0.93 [a]	-	Cloned rat mGluR1	37 °C		
	4.41 ± 1.59 [a]	-	Rat cerebellum homogenate			
	13.3 ± 6.49 [a]	-	Cloned human mGluR1			
2	0.87 ± 0.14 [a]	-	Cloned rat mGluR1	4 °C	3.54 [31]	Rat & Baboon
	1.07 ± 0.38 [a]	-	Rat cerebellum homogenate			
	3.74 ± 1.31 [a]	-	Cloned human mGluR1			
	3.38 ± 1.66 [a]	-	Cloned rat mGluR1	37 °C		
	1.77 ± 1.01 [a]	-	Rat cerebellum homogenate			
	24.7 ± 6.32 [a]	-	Cloned human mGluR1			
3 [^{11}C]YM-202074	4.8 ± 0.37 [b]	-	Rat cerebellum homogenate	25 °C [b]	2.7 [32]	Rat
	-	8.6 ± 0.9 [c]	Cloned human mGluR1	37 °C [c]		
4 [^{11}C]MMTP	7.9 [d]	-	Rat cerebellum homogenate	25 °C [d]	3.15 [33]	Baboon
	-	9.5 [e]	Cloned human mGluR1	37 °C [e]		
5 [^{18}F]MK1312	-	3.6 ± 2.1 [e]	Cloned human mGluR1	37 °C	2.3 [24]	Monkey
6	-	2.6 ± 0.8 [e]	Cloned human mGluR1	37 °C	1.9 [24]	Monkey
7 [^{18}F]FTIDC	-	3.1 ± 0.27 [f]	Cloned mouse mGluR1	37 °C	2.1 [47]	Rat
	-	5.8 ± 0.85 [f]	Cloned rat mGluR1			
	-	5.8 ± 0.49 [f]	Cloned human mGluR1			
8 [^{18}F]FPTQ	14 ± 1.8 [g]	-	Cloned human mGluR1	25 °C	2.53 [38]	Rat
	-	3.6 ± 0.49 [e]	Cloned human mGluR1	37 °C		
9 [^{18}F]FPIT	-	5.4 ± 2.2 [e]	Cloned human mGluR1	37 °C	2.53 [39]	Rat & Monkey
10 [^{18}F]FITM	5.4 ± 1.2 [h]	-	Rat brain homogenate	25 °C	1.46 [41]	Rat & Monkey
	-	5.1 ± 2.0 [e]	Cloned human mGluR1	37 °C		

(Table 2) contd….

Radioligand	Binding affinity (nM)		Membrane	Assay Temperature	Measured log *P* (log *D*)	PET Species
	K_i	IC_{50}				
11 [^{11}C]ITMM	12.6 ± 1.2 [h]	-	Rat brain homogenate	25 °C	2.57 [44]	Rat & Human
12	13.6 ± 3.4 [h]	-	Rat brain homogenate	25 °C	1.74 [48]	Monkey
13 [^{11}C]LY-2428703	-	8.9 [e]	Cloned human mGluR1	37 °C	4.02 [46]	Rat
	0.6 ± 0.05 [i]	-	Rat brain homogenate	25 °C		
	2.1 ± 0.6 [i]	-	Monkey brain homogenate			
	2.7 ± 0.5 [i]	-	Human brain homogenate			

a. Determined in ligand competition binding assays using the radioligand [^{3}H]R214127 [31].

b. Determined in ligand competition binding assays using the radioligand [^{3}H]YM-298198 [49].

c. Inhibition of mGluR1-mediated inositol phosphate production in rat cerebellar granule cells [49].

d. Determined in ligand competition binding assays using the radioligand [^{3}H]MMTP [50].

e. Inhibition of L-glutamate-induced Ca^{2+} mobilization in human mGluR1-expressing CHO cells [24, 40, 50, 51].

f. Inhibition of L-glutamate-induced Ca^{2+} mobilization in human, rat, and mouse mGluR1-expressing CHO cells [47].

g. Determined in ligand competition binding assays using the radioligand [^{3}H]FTIDC [51].

h. Determined in ligand competition binding assays using the radioligand [^{18}F]ITMM [44, 48].

i. Determined in ligand competition binding assays using the radioligand [^{3}H]LSN456066 [46].

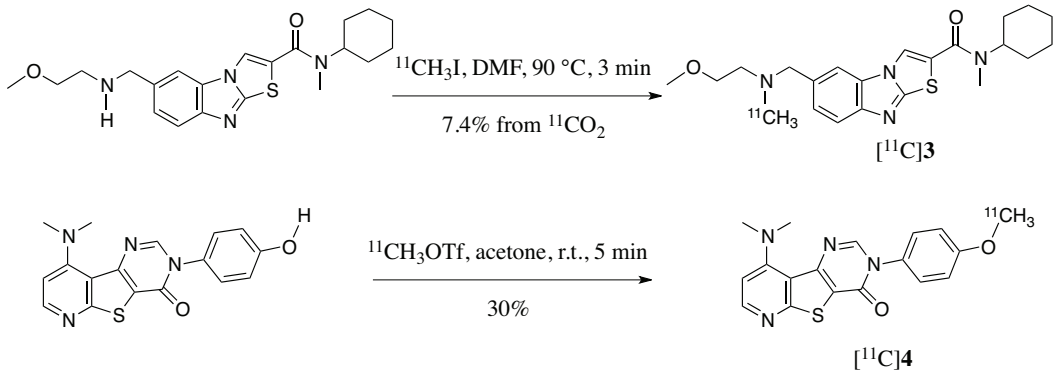

Fig. (3). Radiosynthesis of [^{11}C]**3** and [^{11}C]**4**.

(Table **2**). Ligand **4** was prepared from reaction of the phenol precursor and [^{11}C]methyl triflate in 30% radiochemical yield (EOS, based on [^{11}C]MeOTf) (Fig. **3**). Phosphor imaging autoradiography was performed in postmortem human brain slices and indicated the ability of **4** to label mGluR1 *in vitro*. PET imaging study in a baboon revealed fast uptake and clearance in the brain with a higher concentration of radioactivity in the cerebellum relative to other regions. However, it was not clear whether the binding in the cerebellum was specific, as no blocking study was performed. No further characterization of this radiotracer has been reported since.

In 2009 Merck research laboratories reported in abstract form the preparation of [^{18}F]MK-1312 (**5**) for use in receptor occupancy study of an experimental drug [34]. A full report on this radioligand and a close analog (**6**) was published in 2011 (Fig. **1**) [35]. The radioligands **5** and **6** (IC_{50} of 3.6 and 2.6 nM, respectively, for human mGluR1 in functional assays) were derived from a large series of potent and selective mGluR1 ligands sharing a pyridinyltriazole core structure [36]. The radiolabeling precursors for **5** and **6** were obtained from a 4-step synthesis, and radiosynthesis was carried out with the 2-chloropyridinyltriazole precursors and [^{18}F]fluoride under microwave heating conditions, with F-18 incorporation yield of 46% and 58%, respectively, for **5** and **6** based on HPLC analysis of the crude reaction products (Fig. **4**). Evaluation of the ligands was performed in rhesus monkeys and PET scans indicated a good brain penetration and accumulation of both tracers with the highest uptake in the cerebellum, followed by the thalamus and striatum, in a pattern consistent with the distribution of mGluR1. Although both tracers gave comparable results, tracer **5** appeared to have slightly higher specific binding signals and was further characterized. In the presence of MK-5435, a structurally similar, selective antagonist with IC_{50} of 4.3 nM for human mGluR1 [36], uptake of **5** was reduced in all brain regions in a dose-dependent manner. Correlation of receptor occupancy with MK-5435 plasma concentration gave an EC_{50} (MK-5435 plasma concentration required to inhibit 50% of the tracer's binding) of 76 ± 7 nM. In addition, **5** was used in a saturation binding assays with brain tissue homogenates to derive its *in vitro* dissociation constants (K_d) and mGluR1

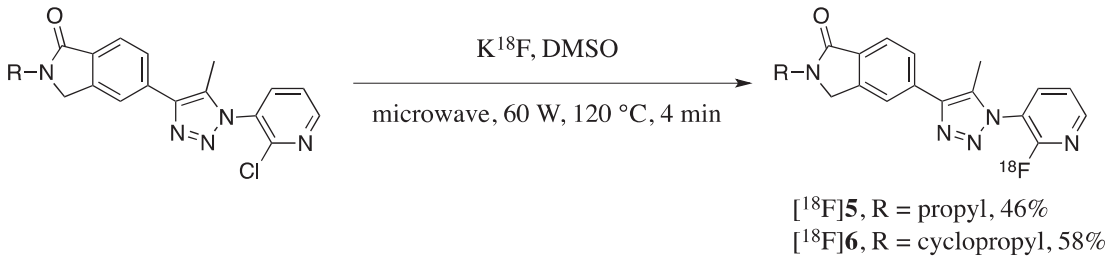

Fig. (4). Radiosynthesis of [^{18}F]**5** and [^{18}F]**6**.

concentrations (B_{max}) in the cerebellum and cortex of rhesus monkey and human. In the cerebellum and cortex of rhesus monky, K_d values of 0.40 and 0.49 nM were obtained, while values of 0.84 and 1.1 nM were obtained in human cerebellum and cortex. Receptor concentrations were listed in Table **1**. Based on the measured B_{max} and K_d values, B_{max}/K_d ratios are 98 and 24, respectively, for human cerebellum and cortex, which is >10, a threshold thought to predict the likelihood of a tracer to give reliably measurable specific binding signal *in vivo*. Hence, **5** may be the first PET tracer suitable for the imaging and quantification of mGluR1 in humans. However, evaluation of **5** in humans has not been reported.

Compounds with the aryltriazole core structures and pioneered by the Merck group were further explored as PET radioligands to image the mGluR1. Among these FTIDC (**7**, Fig. **1**), with an IC_{50} of 5.8 nM for human mGluR1, was labeled with F-18 and evaluated in rodents. Ligand **7** showed high accumulation and specific binding in the thalamus, cerebellum and hippocampus, and thus was claimed to be a promising radioligand for the visualization of mGluR1 [37]. However, results were only disclosed in an abstract form and full details of its *in vivo* evaluation were not available.

Another two ligands from the same aryltriazole chemical scaffold, [^{18}F]FPTQ (**8**) and [^{18}F]FPIT (**9**) (Fig. **1**), were also synthesized and evaluated [38, 39]. Three main fragments: triazole, pyridine and quinoline were brought together through Diels-Alder cycloaddition and Stille coupling with organotin to form the target compounds. Radiolabeling was effected by conventional heating of the 2-bromopyridinyltriazole precursor in DMSO with K^{18}F (Fig. **5**). Decay-corrected radiochemical yield was 69% at EOS for **8**. Radioligand **8** was shown to have high *in vitro* binding affinity, with IC_{50} of 3.6 and 1.4 nM, respectively, for human and mouse mGluR1. PET imaging in rats indicated that **8** displayed regional time activity curves similar to those of [^{11}C]JNJ-16567083 (**1**), with fast uptake and clearance [29, 38]. Self-blocking with unlabeled FPTQ (1 mg/kg) or JNJ-16259685 (1 mg/kg), a selective mGluR1 antagonist, resulted in a homogeneous distribution pattern, while blocking with the mGluR5 antagonist MPEP had no effect, which indicated specific and selective binding of the tracer to mGluR1 in the rat brain. Ligand **8** metabolized rapidly in plasma, with only 4% of parent compound remaining at 30 min post-injection. Further, there appeared to be presence of radioactive metabolites in the rat brain. At 30 min post-injection, parent tracer accounted for 67% of the radioactivity in the cerebellum, and only 34% in the rest of the brain. Given the small specific binding signals in the rat brain, which is at least attributable in part to the presence of radioactive metabolites, there is little prospect for **8** to be a suitable radioligand to image mGluR1 in humans.

Compound **9** (Fig. **1**) in its unlabeled form, with IC_{50} of 5.4 nM for human mGluR1, was first reported by Merck [28, 36]. Fujinaga *et al.* reported the synthesis of **9** in 58% decay-corrected radiochemical yield from its 2-bromopyridinyltriazole precursor (Fig. **5**), since named [^{18}F]FPIT, and evaluated it in rats and rhesus monkeys [39]. In the rat brain [^{18}F]FPIT (**9**) displayed appropriate kinetics and differential uptake among regions in a pattern consistent with the distribution of mGluR1. Further, similar to **8**, its binding appeared to be specific and selective to mGluR1, as pretreatment with unlabeled FPIT or JNJ-16259685 resulted in homogeneous uptake among all brain regions, while pretreatment with MPEP had no effect. Specific binding levels appeared to be high, with peak region of interest (ROI) to medulla uptake ratios of about 3 and 2, respectively, for the cerebellum and thalamus. However, when tested in rhesus monkeys, **9** displayed slow uptake kinetics and spurious binding, as pretreatment with JNJ-16259685 resulted in incomplete blockade of specific binding. Given that self-blocking in rhesus monkey resulted in homogenous regional uptake, and the presence of a small amount of radioactive metabolite (~11% at 90 min post injection) in the rat brain, it was suspected that similar radioactive metabolite(s) might have entered the monkey brain and bound to targets other than mGluR1, which contributed to the incomplete blockade of specific binding by the selective mGluR1 antagonist JNJ-16259685. Consequently, **9** does not constitute a promising ligand to image mGluR1 in humans.

In 2009, Satoh *et al.* reported the discovery of a new class of compounds as potent and selective mGluR1 antagonists, with a central thiazole ring substituted at the 2-position with a substituted benzamide and at the 4-position with substituted pyrimidine [40]. Following this report, Yamasaki *et al.* took one of the most potent and selective compound (IC_{50} = 5.1 nM for mGluR1 and >1,000 selectivity over mGluR2, 5, and 8) and labeled it with F-18 to produce radioligand [^{18}F]FITM (**10**, Fig. **1**) in 14% decay-corrected radiochemical yield (EOS) from the 4-nitrobenzamide precursor (Fig. **6**) [41]. This radioligand was subsequently evaluated *in vivo* in rats and rhesus monkeys [42, 43]. In rats, **10** displayed slow uptake kinetics and a distribution pattern consistent with mGluR1. Binding specificity and selectivity was established by blocking studies with unlabeled FITM, JNJ-16259685 and MPEP. Strong regional specific binding was demonstrated with ROI to pons uptake ratios of about 8 for the cerebellum and 3 to 5 for the thalamus, hippocampus,

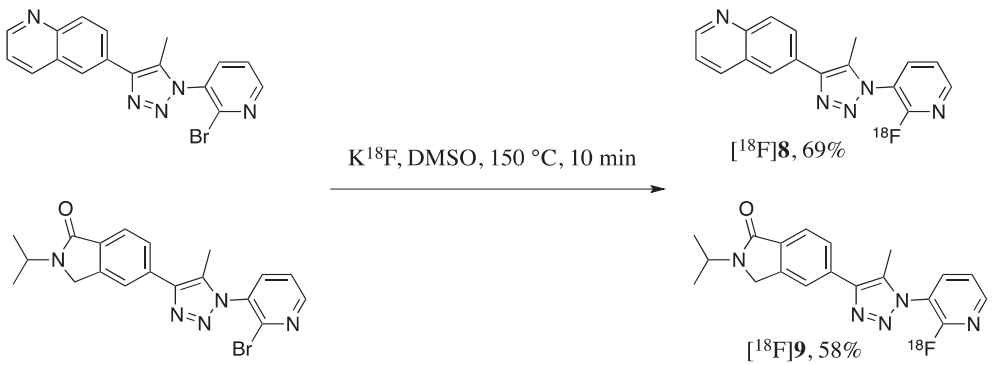

Fig. (5). Radiosynthesis of [^{18}F]**8** and [^{18}F]**9**.

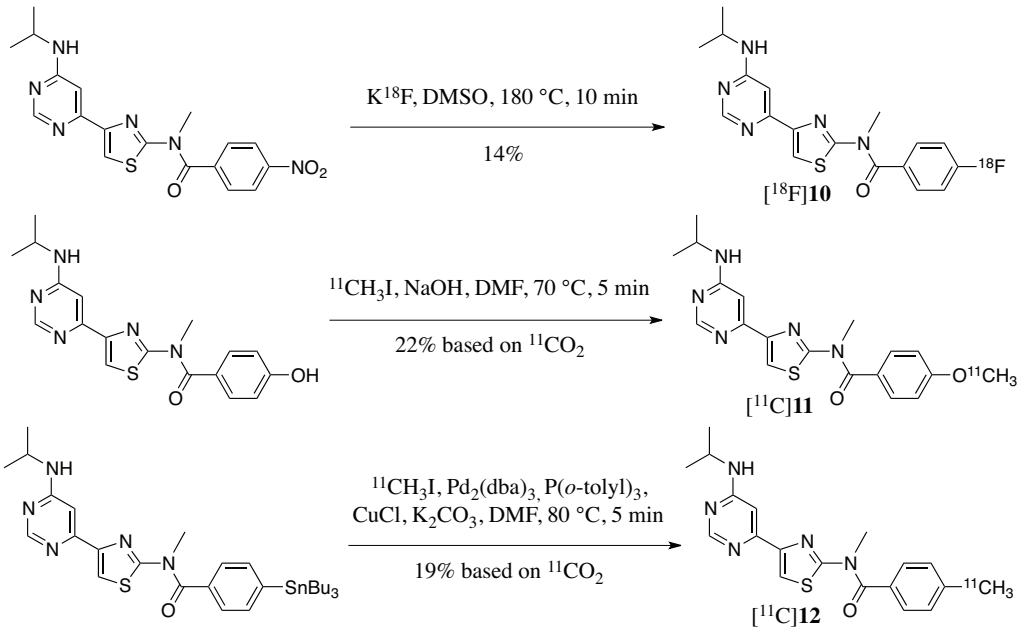

Fig. (6). Radiosynthesis of [^{18}F]**10**, [^{11}C]**11** and [^{11}C]**12**.

striatum and cingulate cortex. Ligand **10** displayed a moderate rate of metabolism with 30.5% of parent fraction in the rat plasma at 30 min post-injection and the presence of two polar metabolites. In the rat brain one radioactive metabolite was detected, but it represented < 5% of the total activity at all time points until the end of the PET scan (120 min), i.e, > 95% of the radioactivity corresponding to the parent tracer.

In rhesus monkeys **10** metabolized at a rate similar to that in rats, with 36.4% of parent fraction remaining at 30 min post-injection and the appearance of two radioactive metabolites in the plasma. In the brain **10** displayed slow kinetics, with little appreciable washout in all regions in the 90 min imaging window. Peak ROI to pons uptake ratios were >3 for the cerebellum, >2 for the cingulate cortex, and 1.5-2 for the thalamus, hippocampus, caudate and putamen. Kinetic parameters were derived with the 2-tissue compartment (2TC) model and Logan graphical analysis. Regional volume of distribution (V_T) values calculated from 2TC analysis were 11.5, 6.0, 5.1, 4.6, 3.4, 3.3 and 2.4 mL/cm^3 for the cerebellum, cingulate cortex, thalamus, hippocampus, putamen, caudate and pons. Given its performance in rhesus monkeys, **10** appears to have the potential to become a promising radioligand for imaging mGluR1 in humans with reliably detectable specific binding signals. However, no report has been published on the evaluation of **10** in humans.

Even though promising results were obtained for **10**, its radiosynthesis was low yielding and purification difficult due to the poor stability of the 4-nitrobenzamide precursor under the reaction conditions. Hence, the same group sought to synthesize and evaluate close structural analogs of **10** with C-11 labeling. Ligand [^{11}C]ITMM (**11**, Fig. **1**), with a methoxy group at the 4-position of the benzamide instead of a fluorine, displayed lower mGluR1 affinity than **10** (*Ki* of 12.6 nM for **11** vs. 5.4 nM for **10**), but retained high selectivity over mGluR5 (IC_{50} > 10,000 nM) [44]. The reference compound and radiolabeling precursor for **11** were prepared in 5 or 6 synthetic steps, respectively, from 4,6-dichloropyrimidine [44]. Radioligand **11** was readily prepared in good radiochemical yield (22% from [^{11}C]CO_2, decay-corrected) and high specific activity (95-140 GBq/μmol, EOS) from its desmethyl precursor and [^{11}C]MeI (Fig. **6**). Two radioligands with 4-[^{18}F]fluoroalkoxy group on the benzamide were also prepared and evaluated along with **11**, but these two F-18 labeled ligands displayed very low affinity for mGluR1 and homogeneous distribution of radioactivity in the rat brain.

In PET imaging experiments in rats the radioligand **11** showed high concentration in the brain, with standard uptake value (SUV) of 2.5 to 3.5 in the cerebellum, thalamus and striatum. Regional specific binding appeared to be high, with peak ROI to pons uptake ratios of 7.0, 5.1 and 4.3, respectively, for the cerebellum, thalamus and striatum. Uptake kinetics was slow, but appreciable washout was observed in all brain regions in the 90-min scan window. Binding specificity and selectivity were demonstrated by blocking studies with the unlabeled parent compound and a selective mGluR1 antagonist (JNJ-16259685, 1 mg/kg each), which resulted in uniformly low uptake in all brain regions. Further studies in wild-type (WT) and mGluR1 knock-out (KO) mice confirmed specific and selective binding of **11** to mGluR1 in the brain, as regional uptake pattern in WT mice was similar to that in the rat brain, while uptake in the KO mice was low and uniform. Recently a first-in-human imaging study was conducted for **11** in one 27-year old male subject [45]. In human, **11** metabolized slowly in the plasma, with 66% and 61% of parent fraction remaining at 30 and 60 min post-injection. Brain uptake was relatively low, with peak SUV of 1-2 among regions, and uptake kinetics was very slow, with a continuing rise of activity in the cerebellum, and little washout in other brain regions in the 90-min scan. Regional time-activity curves were analyzed using a 2-tissue compartment model and the metabolite-corrected arterial plasma concentration curve as input function. Distribution volumes (V_T) were estimated to be 2.7 and 1.1 mL/cm^3 for the cerebellum and thalamus, 0.9, 0.8, 0.7, 0.6 mL/cm^3 for the temporal, parietal, frontal, and occipital cortex; and 0.5 mL/cm^3 for the caudate/putamen. However, given the slow uptake kinetics, it is not clear how reliably these V_T estimates are, and how long a scan may be needed in order to achieve stable estimates of regional V_T.

Replacing the 4-methoxy with 4-methyl group in **11**, a third tracer **12** from this series was prepared using the tributyltinbenzamide precursor in a palladium-catalyzed Stille coupling reaction with [^{11}C]MeI (Fig. **6**). Radiochemical yield of **12** was 19% at EOS (decay-corrected and based on [^{11}C]CO_2). Binding affinity and selectivity of **12** (K_i = 13.6 nM for mGluR1, IC_{50} > 10,000 nM for mGluR5) was similar to **11**. Metabolite analysis indicated a minimal presence of radioactive metabolites in the rat brain, with 94 to 98% of radioactivity representing the parent tracer at all time points, while the parent fraction in the rat plasma decreased to 68%, 48%, 39% and 34% at 5, 15, 30 and 60 min post-injection. In monkeys ligand **12** metabolized at a rate similar to that in rats, with 36 and 28% of parent fraction remaining in the plasma at 30 and 60 min post-injection. Monkey brain uptake of **12** was relatively low, with peak SUV of 0.6 to 1.3 among regions, which were lower than those for **10**. Time-activity curves indicated that the tracer displayed an appropriate kinetics, with clearly defined uptake, peak, and clearance phase in all regions. Pretreatment of the monkeys with the parent compound (1 mg/kg) and a selective mGluR1 antagonist (JNJ-16259685, 3 mg/kg) resulted in homogeneous distribution of radioactivity in all brain regions, an indication of the tracer's binding specificity and selectivity in the monkey brain. Logan reference method was used to derive distribution volume ratios (DVR) with the area under the curve in the blocking scan as an estimate of nondisplaceable binding. DVR was 4.3, 2.6, 2.0, 1.8, and 1.5, respectively, for the cerebellum, cingulate cortex, thalamus, hippocampus, and caudate/putamen.

Finally, the isothiazole derivative [^{11}C]LY-2428703 (**13**) was recently prepared and evaluated as a potential PET tracer for mGluR1 [46]. Ligand **13** displayed an IC_{50} of 8.9 nM for mGluR1 in functional assays and modest selectivity over mGluR5 (IC_{50} = 118 nM). PET imaging experiments in rats indicated a rapid uptake and washout in the brain, with peak cerebellum/forebrain uptake ratio of ~2, similar to that of **1**. Binding specificity was demonstrated by blocking experiment with an mGluR1 antagonist. However, the small specific binding signal displayed by this tracer in rat does not foretell a possibility for it to image mGluR1 in humans.

DISCUSSION

Over the years a number of potent and selective ligands have been investigated as potential PET radiotracers for imaging mGluR1 *in vivo*. None of the early tracers, **1**-**4** (Fig. **1**), appears to have the requisite properties to become useful tracers to image the mGluR1 in humans, due to their limited specific binding signals *in vivo*. For radiotracers coming out of the aryltriazole scaffold (**5**-**9**, Fig. **1**), [^{18}F]MK-1312 (**5**) holds promises as a useful mGluR1 tracer in humans, even though its characterization in humans has not been reported. The most recent addition to the potential mGluR1 radiotracer, [^{11}C]LY-2428703(**13**), also seems to hold little prospect to become a useful imaging agent in humans, given its limited specific binding signals in rats. Hence, within the current collection of mGluR1 radioligands, those derived from the thiazolylbenzamide core structure, **10**-**12**, constitute some of the strong contenders for an effective PET imaging agents for mGluR1 in humans. Among these three tracers, [^{18}F]FITM (**10**) displays slow uptake kinetics, along with high specific binding in regions of the rat and monkey brain. Further advance of this tracer to humans appears to have been abandoned due to chemistry difficulties, i.e., it is difficult to produce the radiotracer in high yield and purity. Tracer [^{11}C]ITMM (**11**), when evaluated in rats, displays uptake kinetics somewhat faster than that of [^{18}F]FITM (**10**), and excellent binding specificity and selectivity. However, when evaluated in a male human subject its uptake kinetics in the cerebellum appears to be irreversible within the 90 min scan window, and very slow in other brain regions. Hence, it may prove difficult to derive reliable kinetic parameters of this tracer within a reasonable scan time (90-120 min) for a C-11 ligand. As for the latest tracer from the thiazolylbenzamide scaffold, **12**, it displays a regional kinetic profile similar to that of [^{18}F]MK-1312 (**5**) in rhesus monkey, with clearly defined uptake, equilibrium and washout phases within the 90 min scan window. Qualitative assessment of regional specific binding signals also reveals similarity between these two tracers. Uptake levels are higher for [^{18}F]MK-1312 (**5**), with peak cerebellum SUV of ~2.5 vs. 1.3 for [^{11}C]**12**. From available data it is predicted that radiotracers [^{18}F]MK-1312 (**5**) and **12** possess the most favorable *in vivo* binding and pharmacokinetic characteristics to become effective PET imaging agents for mGluR1 in humans.

Affinities for mGluR1 and lipophilicity values of all the radiotracers are listed in Table **2**. A survey of the data reveals that, based on the tracer selection criterion of B_{max}/K_D of at least 10 (see above), all tracers are deemed able to provide some measure of specific binding in the rat cerebellum, due to the extremely high level of mGluR1 in this brain region (Table **1**). This is borne out by experimental data. However, tracers **1**-**4**, **7**-**8**, and **13** are inadequate for imaging mGluR5 in higher species, either from actual experimental data in non-human primates, or prediction based on observation of low specific binding signals in rodents. The failure of these radiotracers may be ascribed to a combination of relatively low target affinity, high lipophilicity, and/or the presence of radioactive metabolites in the brain. Two tracers (**5** and **6**) from the aryltriazole class of compounds and three (**10**-**12**) from the substituted thiazolylbenzamide class emerge as PET imaging agents able to produce adequate binding signals in the primate brain. Interestingly, it is from these seemingly success stories that some of the glaring *in vitro-in vivo* inconsistencies are also revealed. For example, tracers **11** and **12**, with *in vitro* K_i of 12.6 and 13.6 nM, respectively, in radioligand competition assays with rat brain homogenates, are calculated to have B_{max}/K_D values of only 4.2 and 3.6 for the monkey cerebellum, far below the threshold of 10 as advocated by Hostetler *et al.* [28], assuming that their *in vitro* K_i values in monkey are similar to those in rat. Hence, they are not predicted to be able to provide high specific binding signals in the primate brain. However, these two tracers actually produce some of the highest binding signals in the primate brain (monkey and human) among the existing ligands. Apparently, the *in vivo* mGluR1 affinities of these two tracers may be much higher than those assayed *in vitro*. These differences between *in vitro* and *in vivo* affinities are not unusual. For example, the *in vitro* K_i of mGluR1 tracer [^{18}F]FITM (**10**) is 5.4 nM, measured in radioligand competition binding assays using rat brain homogenates [44], but its *in vivo* K_d is 1.5 nM in the striatum and cingulate cortex, and 2.1 nM in the hippocampus and thalamus, as derived from PET imaging studies in rats [42]. That is, the *in vivo* affinity of [^{18}F]FITM (**10**) in the rat brain is 2.6 to 3.6 times higher than that measured *in vitro*. This same scenario can happen with tracers **11** and **12**. However, in the absence of experimental data, it is not clear whether the discrepancies arise from the affinity differences between *in vitro* and *in vivo*, or between species, as *in vitro* binding affinities of **11** and **12** were only measured in rat brain homogenates. Determination of *in vitro* affinities of these two ligands in radioligand competition assays using non-human primate tissue homogenates or cloned human mGluR1 will help clarify the situation. An even more definitive answer can be provided with derivation of *in vivo* binding affinities from PET imaging experiments in non-human primates.

Past experience in mGluR1 PET tracer development has indicated that results obtained from rodent studies are poor indicator of a ligand's potential to image and quantitate mGluR1 in humans. This is not surprising, given the substantial species differences in mGluR1 densities (Table **1**) and ligand binding affinities (Table **2**). Therefore, it is our opinion that emerging ligands should be evaluated *in vitro* for binding affinities in radioligand competition assays using cloned human mGluR1, and *in vivo* with PET imaging experiments in non-human primates as soon as possible. Data from these experiments are likely to provide more valid parameters to predict a tracer's success in human, and hence facilitate the advancement of optimal PET tracers to the clinics.

CONCLUSION

The metabotropic glutamate receptor mGluR1 has been implicated in a variety of neuropsychiatric disorders and hence an important target for drug development. As such efforts have been directed toward the development of specific mGluR1 PET radiotracers for use in receptor occupancy studies of experimental therapeutic agents. A number of selective mGluR1 ligands have been prepared and evaluated since early 2000. Initial attempts produced no suitable agents for use in humans. However, in the last two years a few agents have emerged as viable PET ligands for imaging the mGluR1 in humans. Available data indicate that both [^{18}F]MK-1312 (**5**) and **12** display appropriate brain tissue kinetics with well defined phases of uptake, equilibrium and washout, differential uptake among brain regions, and adequate specific binding signals in non-human primates. As regional mGluR1 concentrations in the brain appear to be higher in humans than non-human primates (Table **1**), we predict that these two radiotracers will prove to be suitable mGluR1 PET imaging agents in humans. The availability and application of mGluR1 PET tracers in humans will make it possible to investigate the involvement of this receptor subtype in neurological and psychiatric disorders, and to probe the dose-receptor occupancy relationship of emerging drugs targeting the mGluR1.

CONFLICT OF INTEREST

The authors confirm that this article content has no conflicts of interest.

ACKNOWLEDGEMENTS

Declared none.

REFERENCES

Reference 52 is related article recently published.

[1] Petroff, O.A. GABA and glutamate in the human brain. *Neuroscientist,* **2002**, *8*, 562-573.

[2] Nicoletti, F.; Bockaert, J.; Collingridge, G.L.; Conn, P.J.; Ferraguti, F.; Schoepp, D.D.; Wroblewski, J.T.; Pin, J.P. Metabotropic glutamate receptors: from the workbench to the bedside. *Neuropharmacology,* **2011**, *60*, 1017-1041.

[3] Madden, D.R. The structure and function of glutamate receptor ion channels. *Nat. Rev. Neurosci.,* **2002**, *3*, 91-101.

[4] Palmada, M.; Centelles, J.J. Excitatory amino acid neurotransmission. Pathways for metabolism, storage and reuptake of glutamate in brain. *Front Biosci.,* **1998**, *3*, d701-718.

[5] Nakanishi, S. Molecular diversity of glutamate receptors and implications for brain function. *Science,* **1992**, *258*, 597-603.

[6] Pin, J.P.; Acher, F. The metabotropic glutamate receptors: structure, activation mechanism and pharmacology. *Curr. Drug Targets CNS. Neurol. Disord.,* **2002**, *1*, 297-317.

[7] Houamed, K.M.; Kuijper, J.L.; Gilbert, T.L.; Haldeman, B.A.; O'Hara, P.J.; Mulvihill, E.R.; Almers, W.; Hagen, F.S. Cloning, expression, and gene structure of a G protein-coupled glutamate receptor from rat brain. *Science,* **1991**, *252*, 1318-1321.

[8] Masu, M.; Tanabe, Y.; Tsuchida, K.; Shigemoto, R.; Nakanishi, S. Sequence and expression of a metabotropic glutamate receptor. *Nature,* **1991**, *349*, 760-765.

[9] Lavreysen, H.; Janssen, C.; Bischoff, F.; Langlois, X.; Leysen, J.E.; Lesage, A.S. [^{3}H]R214127: a novel high-affinity radioligand for the mGlu1 receptor reveals a common binding site shared by multiple allosteric antagonists. *Mol. Pharmacol.,* **2003**, *63*, 1082-1093.

[10] Lavreysen, H.; Pereira, S.N.; Leysen, J.E.; Langlois, X.; Lesage, A.S. Metabotropic glutamate 1 receptor distribution and occupancy in the rat brain: a quantitative autoradiographic study using [^{3}H]R214127. *Neuropharmacology,* **2004**, *46*, 609-619.

[11] Bordi, F.; Ugolini, A. Group I metabotropic glutamate receptors: implications for brain diseases. *Prog. Neurobiol.,* **1999**, *59*, 55-79.

[12] Gravius, A.; Pietraszek, M.; Dekundy, A.; Danysz, W. Metabotropic glutamate receptors as therapeutic targets for cognitive disorders. *Curr. Top. Med. Chem.,* **2010**, *10*, 187-206.

[13] Chaki, S.; Hikichi, H. Targeting of metabotropic glutamate receptors for the treatment of schizophrenia. *Curr. Pharm. Des.,* **2011**, *17*, 94-102.

[14] Lesage, A.; Steckler, T. Metabotropic glutamate mGlu1 receptor stimulation and blockade: therapeutic opportunities in psychiatric illness. *Eur. J. Pharmacol.,* **2010**, *639*, 2-16.

[15] Spooren, W.; Ballard, T.; Gasparini, F.; Amalric, M.; Mutel, V.; Schreiber, R. Insight into the function of Group I and Group II metabotropic glutamate (mGlu) receptors: behavioural characterization and implications for the treatment of CNS disorders. *Behav. Pharmacol.,* **2003**, *14*, 257-277.

[16] Frankle, W.G.; Laruelle, M. Neuroreceptor imaging in psychiatric disorders. *Ann. Nucl. Med.,* **2002**, *16*, 437-446.

[17] Newberg, A.B.; Moss, A.S.; Monti, D.A.; Alavi, A. Positron emission tomography in psychiatric disorders. *Ann. N. Y. Acad. Sci.,* **2011**, *1228*, E13-25.

[18] Politis, M.; Piccini, P. Positron emission tomography imaging in neurological disorders. *J. Neurol.,* **2012**, *259*, 1769-1780.

[19] Matthews, P.M.; Rabiner, E.A.; Passchier, J.; Gunn, R.N. Positron emission tomography molecular imaging for drug development. *Br. J. Clin. Pharmacol.,* **2012**, *73*, 175-186.

[20] Huang, Y.; Zheng, M.Q.; Gerdes, J.M. Development of Effective PET and SPECT Imaging Agents for the Serotonin Transporter: Has a Twenty-Year Journey Reached its Destination? *Curr. Top. Med. Chem.,* **2010**, *10*, 1499-1526.

[21] Laruelle, M.; Slifstein, M.; Huang, Y. Relationships between radiotracer properties and image quality in molecular imaging of the brain with positron emission tomography. *Mol. Imaging Biol.,* **2003**, *5*, 363-375.

[22] Pike, V.W. PET radiotracers: crossing the blood-brain barrier and surviving metabolism. *Trends Pharmacol. Sci.,* **2009**, *30*, 431-440.

[23] Heiss, W.D.; Herholz, K. Brain receptor imaging. *J. Nucl. Med.,* **2006**, *47*, 302-312.

[24] Hamill, T.G.; Krause, S.; Ryan, C.; Bonnefous, C.; Govek, S.; Seiders, T.J.; Cosford, N.D.; Roppe, J.; Kamenecka, T.; Patel, S.; Gibson, R.E.; Sanabria, S.; Riffel, K.; Eng, W.; King, C.; Yang, X.; Green, M.D.; O'Malley, S.S.; Hargreaves, R.; Burns, H.D. Synthesis, characterization, and first successful monkey imaging studies of metabotropic glutamate receptor subtype 5 (mGluR5) PET radiotracers. *Synapse,* **2005**, *56*, 205-216.

[25] Eckelman, W.C.; Kilbourn, M.R.; Mathis, C.A. Discussion of targeting proteins *in vivo*: *in vitro* guidelines. *Nucl. Med. Biol.,* **2006**, *33*, 449-451.

[26] Eckelman, W.C.; Mathis, C.A. Targeting proteins *in vivo*: *in vitro* guidelines. *Nucl. Med. Biol.,* **2006**, *33*, 161-164.

[27] Innis, R.B.; Cunningham, V.J.; Delforge, J.; Fujita, M.; Gjedde, A.; Gunn, R.N.; Holden, J.; Houle, S.; Huang, S.C.; Ichise, M.; Iida, H.; Ito, H.; Kimura, Y.; Koeppe, R.A.; Knudsen, G.M.; Knuuti, J.; Lammertsma, A.A.; Laruelle, M.; Logan, J.; Maguire, R.P.; Mintun, M.A.; Morris, E.D.; Parsey, R.; Price, J.C.; Slifstein, M.; Sossi, V.; Suhara, T.; Votaw, J.R.; Wong, D.F.; Carson, R.E. Consensus nomenclature for *in vivo* imaging of reversibly binding radioligands. *J. Cereb. Blood Flow Metab.,* **2007**, *27*, 1533-1539.

[28] Hostetler, E.D.; Eng, W.; Joshi, A.D.; Sanabria-Bohorquez, S.; Kawamoto, H.; Ito, S.; O'Malley, S.; Krause, S.; Ryan, C.; Patel, S.; Williams, M.; Riffel, K.; Suzuki, G.; Ozaki, S.; Ohta, H.; Cook, J.; Burns, H.D.; Hargreaves, R. Synthesis, characterization, and monkey PET studies of [^{18}F]MK-1312, a PET tracer for quantification of mGluR1 receptor occupancy by MK-5435. *Synapse,* **2011**, *65*, 125-135.

[29] Huang, Y.; Narendran, R.; Bischoff, F.; Guo, N.; Zhu, Z.; Bae, S.A.; Lesage, A.S.; Laruelle, M. A positron emission tomography radioligand for the *in vivo* labeling of metabotropic glutamate 1 receptor: (3-Ethyl-2-[^{11}C]methyl-6-quinolinyl)(*cis*-4-methoxycyclohexyl)methanone. *J. Med. Chem.,* **2005**, *48*, 5096-5099.

[30] Mabire, D.; Coupa, S.; Adelinet, C.; Poncelet, A.; Simonnet, Y.; Venet, M.; Wouters, R.; Lesage, A.S.; Van Beijsterveldt, L.; Bischoff, F. Synthesis, structure-activity relationship, and receptor pharmacology of a new series of quinoline derivatives acting as selective, noncompetitive mGlu1 antagonists. *J. Med. Chem.,* **2005**, *48*, 2134-2153.

[31] Huang, Y.; Narendran, R.; Bischoff, F.; Guo, N.; Bae, S.A.; Hwang, D.R.; Lesage, A.S.; Laruelle, M. Synthesis and characterization of two PET radioligands for the metabotropic glutamate 1 (mGlu1) receptor. *Synapse,* **2012**, *66*, 1002-1014.

[32] Yanamoto, K.; Konno, F.; Odawara, C.; Yamasaki, T.; Kawamura, K.; Hatori, A.; Yui, J.; Wakizaka, H.; Nengaki, N.; Takei, M.; Zhang, M.R. Radiosynthesis and evaluation of [^{11}C]YM-202074 as a PET ligand for imaging the metabotropic glutamate receptor type 1. *Nucl. Med. Biol.,* **2010**, *37*, 615-624.

[33] Prabhakaran, J.; Majo, V.J.; Milak, M.S.; Kassir, S.A.; Palner, M.; Savenkova, L.; Mali, P.; Arango, V.; Mann, J.J.; Parsey, R.V.; Kumar, J.S. Synthesis, *in vitro* and *in vivo* evaluation of [^{11}C]MMTP: a potential PET ligand for mGluR1 receptors. *Bioorg. Med. Chem. Lett.,* **2010**, *20*, 3499-3501.

[34] Eng, W.e.a. *In vitro* and *in vivo* characterization of [F-18]MK-1312: a PET tracer for quantification of mGlu1 receptor occupancy by MK-5435. *J. Label. Compd. Radiopharm.,* **2009**, *52*, S84.

[35] Hostetler, E.D.; Eng, W.; Joshi, A.D.; Sanabria-Bohorquez, S.; Kawamoto, H.; Ito, S.; O'Malley, S.; Krause, S.; Ryan, C.; Patel, S.; Williams, M.; Riffel, K.; Suzuki, G.; Ozaki, S.; Ohta, H.; Cook, J.; Burns, H.D.; Hargreaves, R. Synthesis, characterization, and monkey PET studies of [^{18}F]MK-1312, a PET tracer for quantification of mGluR1 receptor occupancy by MK-5435. *Synapse,* **2011**, *65*, 125-135.

[36] Ito, S.; Hirata, Y.; Nagatomi, Y.; Satoh, A.; Suzuki, G.; Kimura, T.; Satow, A.; Maehara, S.; Hikichi, H.; Hata, M.; Ohta, H.; Kawamoto, H. Discovery and biological profile of isoindolinone derivatives as novel metabotropic glutamate receptor 1 antagonists: a potential treatment for psychotic disorders. *Bioorg. Med. Chem. Lett.,* **2009**, *19*, 5310-5313.

[37] Ohgami, M.; Haradahira, T.; Takai, N.; Zhang, M.R.; Kawamura, K.; Yamasaki, T.; Yanagimoto, K. [^{18}F]FTIDC: a new PET radioligand for metabotropic glutamate receptor 1. *Eur. J. Med. Mol. Imaging,* **2009**, *36*, S310.

[38] Fujinaga, M.; Yamasaki, T.; Kawamura, K.; Kumata, K.; Hatori, A.; Yui, J.; Yanamoto, K.; Yoshida, Y.; Ogawa, M.; Nengaki, N.; Maeda, J.; Fukumura, T.; Zhang, M.R. Synthesis and evaluation of 6-[1-(2-[^{18}F]fluoro-3-pyridyl)-5-methyl-1*H*-1,2,3-triazol-4-yl]quinoline for positron emission tomography imaging of the metabotropic glutamate receptor type 1 in brain. *Bioorg. Med. Chem.,* **2011**, *19*, 102-110.

[39] Fujinaga, M.; Maeda, J.; Yui, J.; Hatori, A.; Yamasaki, T.; Kawamura, K.; Kumata, K.; Yoshida, Y.; Nagai, Y.; Higuchi, M.; Suhara, T.; Fukumura, T.; Zhang, M.R. Characterization of 1-(2-[^{18}F]fluoro-3-pyridyl)-4-(2-isopropyl-1-oxo-isoindoline-5-yl)-5-methyl-1*H*-1,2,3-triazole, a PET ligand for imaging the metabotropic glutamate receptor type 1 in rat and monkey brains. *J. Neurochem.,* **2012**, *121*, 115-124.

[40] Satoh, A.; Nagatomi, Y.; Hirata, Y.; Ito, S.; Suzuki, G.; Kimura, T.; Maehara, S.; Hikichi, H.; Satow, A.; Hata, M.; Ohta, H.; Kawamoto, H. Discovery and *in vitro* and *in vivo* profiles of 4-fluoro-*N*-[4-[6-(isopropylamino)pyrimidin-4-yl]-1,3-thiazol-2-yl]-*N*-methylbenzamide as novel class of an orally active metabotropic glutamate receptor 1 (mGluR1) antagonist. *Bioorg. Med. Chem. Lett.,* **2009**, *19*, 5464-5468.

[41] Yamasaki, T.; Fujinaga, M.; Yoshida, Y.; Kumata, K.; Yui, J.; Kawamura, K.; Hatori, A.; Fukumura, T.; Zhang, M.R. Radiosynthesis and preliminary evaluation of 4-[^{18}F]fluoro-*N*-[4-[6-(isopropylamino)pyrimidin-4-yl]-1,3-thiazol-2-yl]-*N*-methylbenzamide as a new positron emission tomography ligand for metabotropic glutamate receptor subtype 1. *Bioorg. Med. Chem. Lett.,* **2011**, *21*, 2998-3001.

[42] Yamasaki, T.; Fujinaga, M.; Kawamura, K.; Yui, J.; Hatori, A.; Ohya, T.; Xie, L.; Wakizaka, H.; Yoshida, Y.; Fukumura, T.; Zhang, M.R. *In vivo* measurement of the affinity and density of me-

tabotropic glutamate receptor subtype 1 in rat brain using ^{18}F-FITM in small-animal PET. *J. Nucl. Med.,* **2012**, *53*, 1601-1607.

[43] Yamasaki, T.; Fujinaga, M.; Maeda, J.; Kawamura, K.; Yui, J.; Hatori, A.; Yoshida, Y.; Nagai, Y.; Tokunaga, M.; Higuchi, M.; Suhara, T.; Fukumura, T.; Zhang, M.R. Imaging for metabotropic glutamate receptor subtype 1 in rat and monkey brains using PET with [^{18}F]FITM. *Eur. J. Nucl. Med. Mol. Imaging,* **2012**, *39*, 632-641.

[44] Fujinaga, M.; Yamasaki, T.; Yui, J.; Hatori, A.; Xie, L.; Kawamura, K.; Asagawa, C.; Kumata, K.; Yoshida, Y.; Ogawa, M.; Nengaki, N.; Fukumura, T.; Zhang, M.R. Synthesis and evaluation of novel radioligands for positron emission tomography imaging of metabotropic glutamate receptor subtype 1 (mGluR1) in rodent brain. *J. Med. Chem.,* **2012**, *55*, 2342-2352.

[45] Toyohara, J.; Sakata, M.; Fujinaga, M.; Yamasaki, T.; Oda, K.; Ishii, K.; Zhang, M.R.; Moriguchi Jeckel, C.M.; Ishiwata, K. Preclinical and the first clinical studies on [^{11}C]ITMM for mapping metabotropic glutamate receptor subtype 1 by positron emission tomography. *Nucl. Med. Biol.,* **2013**, *40*, 214-220.

[46] Zanotti-Fregonara, P.; Barth, V.N.; Liow, J.S.; Zoghbi, S.S.; Clark, D.T.; Rhoads, E.; Siuda, E.; Heinz, B.A.; Nisenbaum, E.; Dressman, B.; Joshi, E.; Luffer-Atlas, D.; Fisher, M.J.; Masters, J.J.; Goebl, N.; Kuklish, S.L.; Morse, C.; Tauscher, J.; Pike, V.W.; Innis, R.B. Evaluation *in vitro* and in animals of a new ^{11}C-labeled PET radioligand for metabotropic glutamate receptors 1 in brain. *Eur. J. Nucl. Med. Mol. Imaging,* **2013**, *40*, 245-253.

[47] Suzuki, G.; Kimura, T.; Satow, A.; Kaneko, N.; Fukuda, J.; Hikichi, H.; Sakai, N.; Maehara, S.; Kawagoe-Takaki, H.; Hata, M.; Azuma, T.; Ito, S.; Kawamoto, H.; Ohta, H. Pharmacological characterization of a new, orally active and potent allosteric metabotropic glutamate receptor 1 antagonist, 4-[1-(2-fluoropyridin-3-yl)-5-methyl-1*H*-1,2,3-triazol-4-yl]-*N*-isopropyl-*N*-methyl-3,6-dihydropyridine-1(2*H*)-carboxamide (FTIDC). *J. Pharmacol. Exp. Ther.,* **2007**, *321*, 1144-1153.

[48] Fujinaga, M.; Yamasaki, T.; Maeda, J.; Yui, J.; Xie, L.; Nagai, Y.; Nengaki, N.; Hatori, A.; Kumata, K.; Kawamura, K.; Zhang, M.R. Development of *N*-[4-[6-(isopropylamino)pyrimidin-4-yl]-1,3-thiazol-2-yl]-*N*-methyl-4-[^{11}C]methylbenzamide for positron emission tomography imaging of metabotropic glutamate 1 receptor in monkey brain. *J. Med. Chem.,* **2012**, *55*, 11042-11051.

[49] Kohara, A.; Takahashi, M.; Yatsugi, S.; Tamura, S.; Shitaka, Y.; Hayashibe, S.; Kawabata, S.; Okada, M. Neuroprotective effects of the selective type 1 metabotropic glutamate receptor antagonist YM-202074 in rat stroke models. *Brain Res.,* **2008**, *1191*, 168-179.

[50] Wu, W.L.; Burnett, D.A.; Domalski, M.; Greenlee, W.J.; Li, C.; Bertorelli, R.; Fredduzzi, S.; Lozza, G.; Veltri, A.; Reggiani, A. Discovery of orally efficacious tetracyclic metabotropic glutamate receptor 1 (mGluR1) antagonists for the treatment of chronic pain. *J. Med. Chem.,* **2007**, *50*, 5550-5553.

[51] Suzuki, G.; Kawagoe-Takaki, H.; Inoue, T.; Kimura, T.; Hikichi, H.; Murai, T.; Satow, A.; Hata, M.; Maehara, S.; Ito, S.; Kawamoto, H.; Ozaki, S.; Ohta, H. Correlation of receptor occupancy of metabotropic glutamate receptor subtype 1 (mGluR1) in mouse brain with *in vivo* activity of allosteric mGluR1 antagonists. *J. Pharmacol. Sci.,* **2009**, *110*, 315-325.

[52] Marmiroli, P.; Cavaletti, G. The glutamatergic neurotransmission in the central nervous system. *Curr. Med. Chem*., **2012**, *19*(9), 1269-1276

Received: May 02, 2013 **Revised: June 17, 2013** **Accepted: July 14, 2013**